



Designation: E1921 – 20

# Standard Test Method for Determination of Reference Temperature, $T_o$ , for Ferritic Steels in the Transition Range<sup>1</sup>

This standard is issued under the fixed designation E1921; the number immediately following the designation indicates the year of original adoption or, in the case of revision, the year of last revision. A number in parentheses indicates the year of last reapproval. A superscript epsilon ( $\epsilon$ ) indicates an editorial change since the last revision or reapproval.

## 1. Scope

1.1 This test method covers the determination of a reference temperature,  $T_o$ , which characterizes the fracture toughness of ferritic steels that experience onset of cleavage cracking at elastic, or elastic-plastic  $K_{Jc}$  instabilities, or both. The specific types of ferritic steels (3.2.2) covered are those with yield strengths ranging from 275 to 825 MPa (40 to 120 ksi) and weld metals, after stress-relief annealing, that have 10 % or less strength mismatch relative to that of the base metal.

1.2 The specimens covered are fatigue precracked single-edge notched bend bars, SE(B), and standard or disk-shaped compact tension specimens, C(T) or DC(T). A range of specimen sizes with proportional dimensions is recommended. The dimension on which the proportionality is based is specimen thickness.

1.3 Median  $K_{Jc}$  values tend to vary with the specimen type at a given test temperature, presumably due to constraint differences among the allowable test specimens in 1.2. The degree of  $K_{Jc}$  variability among specimen types is analytically predicted to be a function of the material flow properties (1)<sup>2</sup> and decreases with increasing strain hardening capacity for a given yield strength material. This  $K_{Jc}$  dependency ultimately leads to discrepancies in calculated  $T_o$  values as a function of specimen type for the same material.  $T_o$  values obtained from C(T) specimens are expected to be higher than  $T_o$  values obtained from SE(B) specimens. Best estimate comparisons of several materials indicate that the average difference between C(T) and SE(B)-derived  $T_o$  values is approximately 10°C (2). C(T) and SE(B)  $T_o$  differences up to 15 °C have also been recorded (3). However, comparisons of individual, small datasets may not necessarily reveal this average trend. Datasets which contain both C(T) and SE(B) specimens may generate  $T_o$  results which fall between the  $T_o$  values calculated using solely C(T) or SE(B) specimens. It is therefore strongly

recommended that the specimen type be reported along with the derived  $T_o$  value in all reporting, analysis, and discussion of results. This recommended reporting is in addition to the requirements in 11.1.1.

1.4 Requirements are set on specimen size and the number of replicate tests that are needed to establish acceptable characterization of  $K_{Jc}$  data populations.

1.5  $T_o$  is dependent on loading rate.  $T_o$  is evaluated for a quasi-static loading rate range with  $0.1 < dK/dt < 2$  MPa√m/s. Slowly loaded specimens ( $dK/dt < 0.1$  MPa√m) can be analyzed if environmental effects are known to be negligible. Provision is also made for higher loading rates ( $dK/dt > 2$  MPa√m/s) in Annex A1. Note that this threshold loading rate for application of Annex A1 is a much lower threshold than is required in other fracture toughness test methods such as E399 and E1820.

1.6 The statistical effects of specimen size on  $K_{Jc}$  in the transition range are treated using the weakest-link theory (4) applied to a three-parameter Weibull distribution of fracture toughness values. A limit on  $K_{Jc}$  values, relative to the specimen size, is specified to ensure high constraint conditions along the crack front at fracture. For some materials, particularly those with low strain hardening, this limit may not be sufficient to ensure that a single-parameter ( $K_{Jc}$ ) adequately describes the crack-front deformation state (5).

1.7 Statistical methods are employed to predict the transition toughness curve and specified tolerance bounds for 1T specimens of the material tested. The standard deviation of the data distribution is a function of Weibull slope and median  $K_{Jc}$ . The procedure for applying this information to the establishment of transition temperature shift determinations and the establishment of tolerance limits is prescribed.

1.8 The procedures described in this test method assume that the data set represents a macroscopically homogeneous material, such that the test material has uniform tensile and toughness properties. Application of this test method to an inhomogeneous material will result in an inaccurate estimate of the transition reference value  $T_o$  and nonconservative confidence bounds. For example, multi-pass weldments can create heat-affected and brittle zones with localized properties that are

<sup>1</sup> This test method is under the jurisdiction of ASTM Committee E08 on Fatigue and Fracture and is the direct responsibility of E08.07 on Fracture Mechanics.

Current edition approved June 1, 2020. Published August 2020. Originally approved in 1997. Last previous edition approved in 2019 as E1921 – 19b<sup>ε1</sup>. DOI: 10.1520/E1921-20.

<sup>2</sup> The boldface numbers in parentheses refer to the list of references at the end of this standard.

quite different from either the bulk or weld materials. Thick-section steels also often exhibit some variation in properties near the surfaces. Metallography and initial screening may be necessary to verify the applicability of these and similarly graded materials. Section 10.6 provides a screening criterion to assess whether the data set may not be representative of a macroscopically homogeneous material, and therefore, may not be amenable to the statistical analysis procedures employed in this test method. If the data set fails the screening criterion in 10.6, the homogeneity of the material and its fracture toughness can be more accurately assessed using the analysis methods described in Appendix X5.

1.9 This standard does not purport to address all of the safety concerns, if any, associated with its use. It is the responsibility of the user of this standard to establish appropriate safety, health, and environmental practices and determine the applicability of regulatory limitations prior to use.

1.10 This international standard was developed in accordance with internationally recognized principles on standardization established in the Decision on Principles for the Development of International Standards, Guides and Recommendations issued by the World Trade Organization Technical Barriers to Trade (TBT) Committee.

## 2. Referenced Documents

### 2.1 ASTM Standards:<sup>3</sup>

- E4 Practices for Force Verification of Testing Machines
  - E8/E8M Test Methods for Tension Testing of Metallic Materials
  - E23 Test Methods for Notched Bar Impact Testing of Metallic Materials
  - E74 Practices for Calibration and Verification for Force-Measuring Instruments
  - E111 Test Method for Young's Modulus, Tangent Modulus, and Chord Modulus
  - E177 Practice for Use of the Terms Precision and Bias in ASTM Test Methods
  - E208 Test Method for Conducting Drop-Weight Test to Determine Nil-Ductility Transition Temperature of Ferritic Steels
  - E399 Test Method for Linear-Elastic Plan-Strain Fracture Toughness  $K_{Ic}$  of Metallic Materials
  - E436 Test Method for Drop-Weight Tear Tests of Ferritic Steels
  - E561 Test Method for  $K_R$  Curve Determination
  - E691 Practice for Conducting an Interlaboratory Study to Determine the Precision of a Test Method
  - E1820 Test Method for Measurement of Fracture Toughness
  - E1823 Terminology Relating to Fatigue and Fracture Testing
- ### 2.2 ASME Standards:<sup>4</sup>
- ASME Boiler and Pressure Vessel Code, Section II, Part D

<sup>3</sup> For referenced ASTM standards, visit the ASTM website, [www.astm.org](http://www.astm.org), or contact ASTM Customer Service at [service@astm.org](mailto:service@astm.org). For *Annual Book of ASTM Standards* volume information, refer to the standard's Document Summary page on the ASTM website.

<sup>4</sup> Available from American Society of Mechanical Engineers (ASME), ASME International Headquarters, Two Park Ave., New York, NY 10016-5990, <http://www.asme.org>.

## 3. Terminology

3.1 Terminology given in Terminology E1823 is applicable to this test method.

### 3.2 Definitions:

3.2.1 *effective yield strength*,  $\sigma_Y$  [ $FL^{-2}$ ]*—* an assumed value of uniaxial yield strength that represents the influence of plastic yielding upon fracture test parameters.

3.2.1.1 *Discussion—*It is calculated as the average of the 0.2 % offset yield strength  $\sigma_{YS}$ , and the ultimate tensile strength,  $\sigma_{TS}$  as follows:

$$\sigma_Y = \frac{\sigma_{YS} + \sigma_{TS}}{2}$$

3.2.2 *ferritic steels—*typically carbon, low-alloy, and higher alloy grades. Typical microstructures are bainite, tempered bainite, tempered martensite, and ferrite and pearlite. All ferritic steels have body centered cubic crystal structures that display ductile-to-cleavage transition temperature fracture toughness characteristics. See also Test Methods E23, E208 and E436.

3.2.2.1 *Discussion—*This definition is not intended to imply that all of the many possible types of ferritic steels have been verified as being amenable to analysis by this test method.

3.2.3 *stress-intensity factor*,  $K$  [ $FL^{-3/2}$ ]*—*the magnitude of the mathematically ideal crack-tip stress field coefficient (stress field singularity) for a particular mode of crack-tip region deformation in a homogeneous body.

3.2.3.1 *Discussion—*In this test method, Mode I is assumed. See Terminology E1823 for further discussion.

3.2.4 *J-integral*,  $J$  [ $FL^{-1}$ ]*—*a mathematical expression; a line or surface integral that encloses the crack front from one crack surface to the other; used to characterize the local stress-strain field around the crack front (6). See Terminology E1823 for further discussion.

### 3.3 Definitions of Terms Specific to This Standard:

3.3.1 *control force*,  $P_m$  [ $F$ ]*—*a calculated value of maximum force, used in 7.8.1 to stipulate allowable precracking limits.

3.3.2 *crack initiation—*describes the onset of crack propagation from a preexisting macroscopic crack created in the specimen by a stipulated procedure.

3.3.3 *effective modulus*,  $E_{eff}$  [ $FL^{-2}$ ]*—*an elastic modulus that allows a theoretical (modulus normalized) compliance to match an experimentally measured compliance for an actual initial crack size,  $a_o$ .

3.3.4 *elastic modulus*,  $E'$  [ $FL^{-2}$ ]*—*a linear-elastic factor relating stress to strain, the value of which is dependent on the degree of constraint. For plane stress,  $E' = E$  is used, and for plane strain,  $E/(1 - \nu^2)$  is used, with  $E$  being Young's modulus and  $\nu$  being Poisson's ratio.

3.3.5 *elastic plastic  $J_c$*  [ $FL^{-1}$ ]*—* $J$ -integral at the onset of cleavage fracture.

3.3.6 *elastic-plastic  $K_J$*  [ $FL^{-3/2}$ ]*—*An elastic-plastic equivalent stress intensity factor derived from the  $J$ -integral.

3.3.6.1 *Discussion—*In this test method,  $K_J$  also implies a

stress intensity factor determined at the test termination point under conditions that require censoring the data by 8.9.2.

3.3.7 *elastic-plastic  $K_{Jc}$  [ $FL^{-3/2}$ ]*—an elastic-plastic equivalent stress intensity factor derived from the  $J$ -integral at the point of onset of cleavage fracture,  $J_c$ .

3.3.8 *equivalent value of median toughness,  $K_{Jc(med)}^{eq}$  [ $FL^{-3/2}$ ]*—an equivalent value of the median toughness for a multi-temperature data set.

3.3.9 *Eta ( $\eta$ )*—a dimensionless parameter that relates plastic work done on a specimen to crack growth resistance defined in terms of deformation theory  $J$ -integral (7).

3.3.10 *failure probability,  $p_f$* —the probability that a single selected specimen chosen at random from a population of specimens will fail at or before reaching the  $K_{Jc}$  value of interest.

3.3.11 *initial ligament length,  $b_o$  [ $L$ ]*—the distance from the initial crack tip,  $a_o$ , to the back face of a specimen.

3.3.12 *load-line displacement rate,  $\dot{\Delta}_{LL}$  [ $LT^{-1}$ ]*—rate of increase of specimen load-line displacement.

3.3.13 *pop-in*—a discontinuity in a force versus displacement test record (8).

3.3.13.1 *Discussion*—A pop-in event is usually audible, and is a sudden cleavage crack initiation event followed by crack arrest. The test record will show increased displacement and drop in applied force if the test frame is stiff. Subsequently, the test record may continue on to higher forces and increased displacements.

3.3.14 *precracked Charpy, PCC, specimen*—SE(B) specimen with  $W = B = 10$  mm (0.394 in.).

3.3.15 *provisional reference temperature, ( $T_{oQ}$ ) [ $^{\circ}C$ ]*—Interim  $T_o$  value calculated using the standard test method described herein.  $T_{oQ}$  is validated as  $T_o$  in 10.5.

3.3.16 *reference temperature,  $T_o$  [ $^{\circ}C$ ]*—The test temperature at which the median of the  $K_{Jc}$  distribution from 1T size specimens will equal 100 MPa $\sqrt{m}$  (91.0 ksi $\sqrt{in.}$ ).

3.3.17 *SE(B) specimen span,  $S$  [ $L$ ]*—the distance between specimen supports (See Test Method E1820 Fig. 3).

3.3.18 *specimen thickness,  $B$  [ $L$ ]*—the distance between the parallel sides of a test specimen as depicted in Fig. 1–3.

3.3.18.1 *Discussion*—In the case of side-grooved specimens, the net thickness,  $B_N$ , is the distance between the roots of the side-groove notches.

3.3.19 *specimen size,  $nT$* —a code used to define specimen dimensions, where  $n$  is expressed in multiples of 1 in.

3.3.19.1 *Discussion*—In this method, specimen proportionality is required. For compact specimens and bend bars, specimen thickness  $B = n$  inches.

3.3.20 *temperature,  $T_Q$  [ $^{\circ}C$ ]*—For  $K_{Jc}$  values that are developed using specimens or test practices, or both, that do not conform to the requirements of this test method, a temperature at which  $K_{Jc(med)} = 100$  MPa $\sqrt{m}$  is defined as  $T_Q$ .  $T_Q$  is not a provisional value of  $T_o$ .

3.3.21 *time to control force,  $t_m$  [ $T$ ]*—time to  $P_m$ .

3.3.22 *Weibull fitting parameter,  $K_o$* —a scale parameter located at the 63.2 % cumulative failure probability level (9).  $K_{Jc} = K_o$  when  $p_f = 0.632$ .

3.3.23 *Weibull slope,  $b$* —with  $p_f$  and  $K_{Jc}$  data pairs plotted in linearized Weibull coordinates obtainable by rearranging Eq 18,  $b$  is the slope of a line that defines the characteristics of the typical scatter of  $K_{Jc}$  data.

3.3.23.1 *Discussion*—A Weibull slope of 4 is used exclusively in this method.

3.3.24 *yield strength,  $\sigma_{YS}$  [ $FL^{-2}$ ]*—the stress at which a material exhibits a specific limiting deviation from the proportionality of stress to strain at the test temperature. This deviation is expressed in terms of strain.

3.3.24.1 *Discussion*—It is customary to determine yield strength by either (1) Offset Method (usually a strain of 0.2 % is specified) or (2) Total-Extension-Under-Force Method (usually a strain of 0.5 % is specified although other values of strain may be used).

3.3.24.2 *Discussion*—Whenever yield strength is specified, the method of test must be stated along with the percent offset or total strain under force. The values obtained by the two methods may differ.

## 4. Summary of Test Method

4.1 This test method involves the testing of notched and fatigue precracked bend or compact specimens in a temperature range where either cleavage cracking or crack pop-in develop during the loading of specimens. Crack aspect ratio,  $a/W$ , is nominally 0.5. Specimen width in compact specimens is two times the thickness. In bend bars, specimen width can be either one or two times the thickness.

4.2 Force versus displacement across the notch at a specified location is recorded by autographic recorder or computer data acquisition, or both. Fracture toughness is calculated at a defined condition of crack instability. The  $J$ -integral value at instability,  $J_c$ , is calculated and converted into its equivalent in units of stress intensity factor,  $K_{Jc}$ . Censoring limits are based on  $K_{Jc}$  to determine the suitability of data for statistical analyses.

4.3 A minimum of six tests are required to estimate the median  $K_{Jc}$  of the Weibull distribution for the data population (10). Extensive data scatter among replicate tests is expected. Statistical methods are used to characterize these data populations and to predict changes in data distributions with changed specimen size.

4.4 The statistical relationship between specimen size and  $K_{Jc}$  fracture toughness is assessed using weakest-link theory, thereby providing a relationship between the specimen size and  $K_{Jc}$  (4). Limits are placed on the fracture toughness range over which this model can be used.

4.5 For the definition of the toughness transition curve, a master curve concept is used (11, 12). The position of the curve on the temperature coordinate is established from the experimental determination of the temperature, designated  $T_o$ , at which the median  $K_{Jc}$  for 1T size specimens is 100 MPa $\sqrt{m}$  (91.0 ksi $\sqrt{in.}$ ). Selection of a test temperature close to that at which the median  $K_{Jc}$  value will be 100 MPa $\sqrt{m}$  is encouraged.

and a means of estimating this temperature is suggested. Small specimens such as precracked Charpy's may have to be tested at temperatures below  $T_o$  where  $K_{Jc(med)}$  is well below 100 MPa $\sqrt{m}$ . In such cases, additional specimens may be required as stipulated in 8.5.

4.6 Tolerance bounds can be determined that define the range of scatter in fracture toughness throughout the transition range.

## 5. Significance and Use

5.1 Fracture toughness is expressed in terms of an elastic-plastic stress intensity factor,  $K_{Jc}$ , that is derived from the  $J$ -integral calculated at fracture.

5.2 Ferritic steels are microscopically inhomogeneous with respect to the orientation of individual grains. Also, grain boundaries have properties distinct from those of the grains. Both contain carbides or nonmetallic inclusions that can act as nucleation sites for cleavage microcracks. The random location of such nucleation sites with respect to the position of the crack front manifests itself as variability of the associated fracture toughness (13). This results in a distribution of fracture toughness values that is amenable to characterization using the statistical methods in this test method.

5.3 The statistical methods in this test method assume that the data set represents a macroscopically homogeneous material, such that the test material has both the uniform tensile and toughness properties. The fracture toughness evaluation of nonuniform materials is not amenable to the statistical analysis procedures employed in this test method. For example, multipass weldments can create heat-affected and brittle zones with localized properties that are quite different from either the bulk or weld materials. Thick-section steels also often exhibit some variation in properties near the surfaces. Metallographic analysis can be used to identify possible nonuniform regions in a material. These regions can then be evaluated through mechanical testing such as hardness, microhardness, and tensile testing for comparison with the bulk material. It is also advisable to measure the toughness properties of these nonuniform regions distinctly from the bulk material. Section 10.6 provides a screening criterion to assess whether the data set may not be representative of a macroscopically homogeneous material, and therefore, may not be amenable to the statistical analysis procedures employed in this test method. If the data set fails the screening criterion in 10.6, the homogeneity of the material and its fracture toughness can be more accurately assessed using the analysis methods described in Appendix X5.

5.4 Distributions of  $K_{Jc}$  data from replicate tests can be used to predict distributions of  $K_{Jc}$  for different specimen sizes. Theoretical reasoning (9), confirmed by experimental data, suggests that a fixed Weibull slope of 4 applies to all data distributions and, as a consequence, standard deviation on data scatter can be calculated. Data distribution and specimen size effects are characterized using a Weibull function that is coupled with weakest-link statistics (14). An upper limit on constraint loss and a lower limit on test temperature are defined between which weakest-link statistics can be used.

5.5 The experimental results can be used to define a master curve that describes the shape and location of median  $K_{Jc}$  transition temperature fracture toughness for 1T specimens (15). The curve is positioned on the abscissa (temperature coordinate) by an experimentally determined reference temperature,  $T_o$ . Shifts in reference temperature are a measure of transition temperature change caused, for example, by metallurgical damage mechanisms.

5.6 Tolerance bounds on  $K_{Jc}$  can be calculated based on theory and generic data. For added conservatism, an offset can be added to tolerance bounds to cover the uncertainty associated with estimating the reference temperature,  $T_o$ , from a relatively small data set. From this it is possible to apply a margin adjustment to  $T_o$  in the form of a reference temperature shift.

5.7 For some materials, particularly those with low strain hardening, the value of  $T_o$  may be influenced by specimen size due to a partial loss of crack-tip constraint (5). When this occurs, the value of  $T_o$  may be lower than the value that would be obtained from a data set of  $K_{Jc}$  values derived using larger specimens.

5.8 As discussed in 1.3, there is an expected bias among  $T_o$  values as a function of the standard specimen type. The magnitude of the bias may increase inversely to the strain hardening ability of the test material at a given yield strength, as the average crack-tip constraint of the data set decreases (16). On average,  $T_o$  values obtained from C(T) specimens are higher than  $T_o$  values obtained from SE(B) specimens. Best estimate comparison indicates that the average difference between C(T) and SE(B)-derived  $T_o$  values is approximately 10 °C (2). However, individual C(T) and SE(B) datasets may show much larger  $T_o$  differences (3, 17, 18), or the SE(B)  $T_o$  values may be higher than the C(T) values (2). On the other hand, comparisons of individual, small datasets may not necessarily reveal this average trend. Datasets which contain both C(T) and SE(B) specimens may generate  $T_o$  results which fall between the  $T_o$  values calculated using solely C(T) or SE(B) specimens.

## 6. Apparatus

6.1 *Precision of Instrumentation*—Measurements of applied forces and load-line displacements are needed to obtain work done on the specimen. Force versus load-line displacement shall be recorded digitally on computers or autographically on  $x$ - $y$  plotters. For computers, digital signal resolution shall be at least 1/32,000 of the displacement transducer signal range and shall be at least 1/4,000 of the force transducer signal range.

6.2 *Grips for C(T) Specimens*—A clevis with flat-bottom holes is recommended. See Test Method E399, Fig. A6.2, for a recommended design. Clevises and pins should be fabricated from steels of sufficient strength to elastically resist indentation loads (greater than 40 Rockwell hardness C scale (HRC)).

6.3 *Bend Test Fixture*—A suitable bend test fixture scheme is shown in Fig. A3.2 of Test Method E399. It allows for roller pin rotation and minimizes friction effects during the test. Fixturing and rolls should be made of high-hardness steel (HRC greater than 40).

#### 6.4 *Displacement Gage for Compact Specimens:*

6.4.1 Displacement measurements are made so that  $J$  values are determined from area under force versus displacement test records (a measure of work done). If the test temperature selection recommendations of this practice are followed, crack growth measurement will probably prove to be unimportant. Results that fall within the limits of uncertainty of the recommended test temperature estimation scheme will probably not have significant slow-stable crack growth prior to instability. Nevertheless, crack growth measurements are recommended to provide supplementary information, and these results may be reported.

6.4.2 Unloading compliance is the primary recommendation for measuring slow-stable crack growth. See Test Method E1820. When multiple tests are performed sequentially at low test temperatures, there will be condensation and ice buildup on the grips between the loading pins and flats of the clevis holes. Ice will interfere with the accuracy of the unloading compliance method. Alternatively, crack growth can be measured by other methods such as electric potential, but care must be taken to avoid specimen heating when low test temperatures are used.

6.4.3 In compact C(T) specimens, displacement measurements on the load-line are recommended for  $J$  determinations. However, the front face position at  $0.25W$  in front of the load-line can be used with interpolation to load-line displacement, as suggested in 7.1.

6.4.4 Clip gage (or other similar displacement gage) accuracy shall be verified according to 6.2.2 of Test Method E1820.

#### 6.5 *Displacement Gages for Bend Bars, SE(B):*

6.5.1 The SE(B) specimen has two displacement gage locations. A load-line displacement transducer is primarily intended for  $J$  computation, but may also be used for calculations of crack size based on elastic compliance, if provision is made to subtract the extra displacement due to the elastic compliance of the fixturing. The load-line gage shall display accuracy of 1 % over the working range of the gage. The gages used shall not be temperature sensitive.

6.5.2 Alternatively, a crack-mouth opening displacement (CMOD) gage can also be used to determine the plastic part of  $J$ . However, it is necessary to employ a plastic  $\eta$  value developed specifically for the CMOD location (19) or infer load-point displacement from CMOD using an expression that relates the two displacements (20). In either case, the procedure described in 9.1.4 is used to calculate the plastic part of  $J$ . However, it is recommended that the plastic part of  $J$  be estimated from the direct CMOD or load-line displacement measurement rather than inferring load-line displacement from CMOD. Additionally, CMOD measurement is more accurate than load-line displacement for estimating crack length from compliance.

6.5.3 Crack growth can be measured by alternative methods such as electric potential, but care must be taken to minimize specimen heating effects in low-temperature tests (see also 6.4.2) (21).

#### 6.6 *Force Measurement:*

6.6.1 Testing shall be performed in a machine conforming to Practices of E4 and Test Methods E8/E8M. Applied force may

be measured by any transducer with a noise-to-signal ratio less than 1/2,000 of the transducer signal range.

6.6.2 Calibrate force measurement instruments by way of Practice E74, 10.2. Annual calibration using calibration equipment traceable to the National Institute of Standards and Technology is a mandatory requirement.

6.7 *Temperature Control*—Specimen temperature shall be measured with thermocouple wires and potentiometers. It is recommended that the two thermocouple wires be attached to the specimen surface separately, either by welding, spot welding, or by being affixed mechanically. Mechanical attachment schemes must be verified to provide equivalent temperature measurement accuracy. The purpose is to use the test material as a part of the thermocouple circuit (see also 8.6.1). Accuracy of temperature measurement shall be within 3°C of true temperature and repeatability among specimens shall be within 2°C. Precision of measurement shall be  $\pm 1^\circ\text{C}$  or better. The temperature measuring apparatus shall be checked every six months using instruments traceable to the National Institute of Standards and Technology in order to ensure the required accuracy.

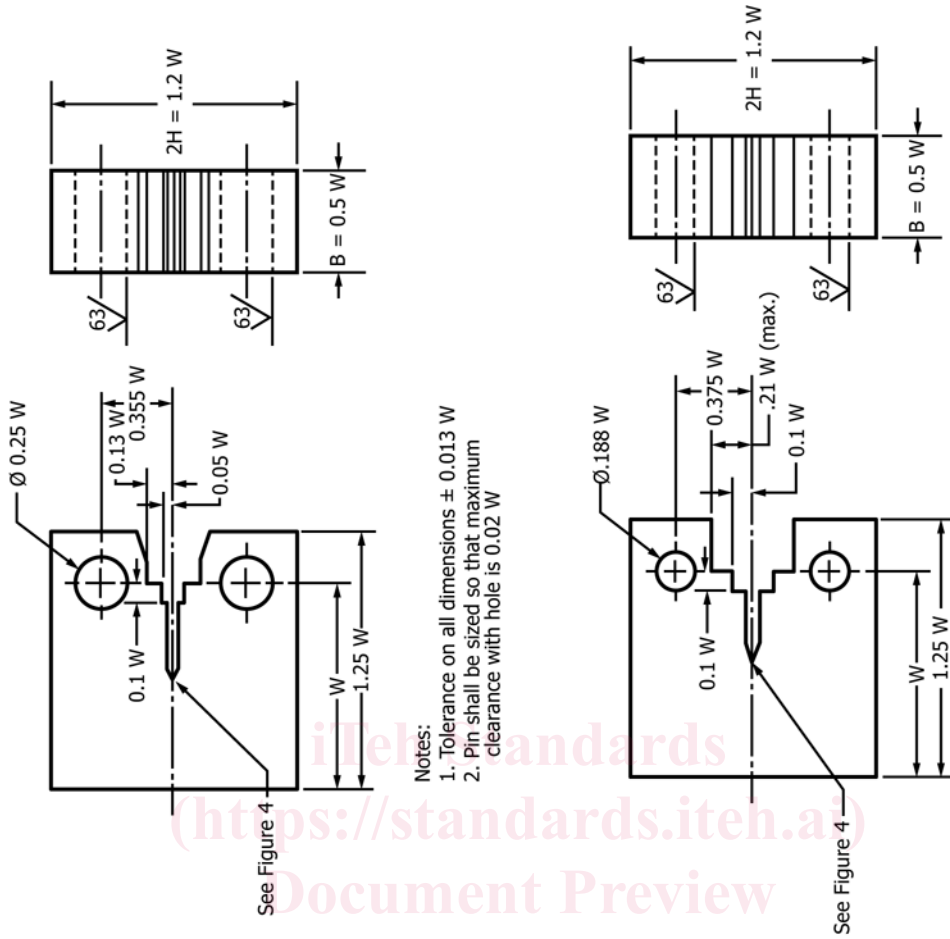
## 7. Specimen Configuration, Dimensions, and Preparation

7.1 *Compact Specimens*—Three recommended C(T) specimen designs are shown in Fig. 1. One C(T) specimen configuration is taken from Test Method E399; the two with cutout sections are taken from E1820. The latter two designs are modified to permit load-line displacement measurement. Room is provided for attachment of razor blade tips on the load-line. Care should be taken to maintain parallel alignment of the blade edges. When front face (at  $0.25W$  in front of the load-line) displacement measurements are made with the Test Method E399 design, the load-line displacement can be inferred by multiplying the measured values by the constant 0.73 (22). The ratio of specimen height to width,  $2H/W$  is 1.2, and this ratio is to be the same for all types and sizes of C(T) specimens. The initial crack size,  $a_o$ , shall be  $0.5W \pm 0.05W$ . Specimen width,  $W$ , shall be  $2B$ .

7.2 *Disk-shaped Compact Specimens*—A recommended DC(T) specimen design is shown in Fig. 2. Initial crack size,  $a_o$ , shall be  $0.5W \pm 0.05W$ . Specimen width shall be  $2B$ .

7.3 *Single-edge Notched Bend*—The recommended SE(B) specimen designs, shown in Fig. 3, are made for use with a span-to-width ratio,  $S/W = 4$ . The width,  $W$ , can be either  $1B$  or  $2B$ . The initial crack size,  $a_o$ , shall be  $0.5W \pm 0.05W$ .

7.4 *Machined Notch Design*—Three designs of fatigue crack starter notches are shown in Fig. 4. These notches can be straight through the specimen thickness or incorporate the chevron form (Fig. 4). To facilitate fatigue cracking at low stress intensity levels, it is recommended that the root radius for either a straight-through slot terminating in a V-notch, or a narrow notch, be 0.08 mm (0.003 in.) or less. If a chevron form of notch is used, the root radius may be 0.25 mm (0.010 in.) or less. In the case of a notch ending in a drilled hole, a sharp stress raiser at the end of the hole will facilitate fatigue precracking and help ensure that the precrack centering requirement in 7.8.2 is met.

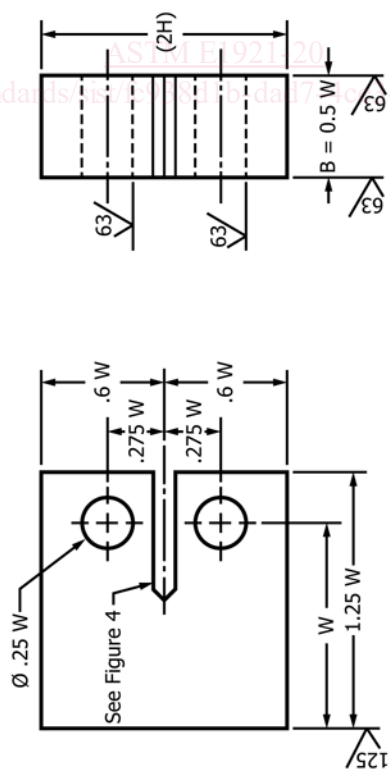


See Figure 4

See Figure 4

- Notes:
1. Tolerance on all dimensions  $\pm 0.013 W$
  2. Pin shall be sized so that maximum clearance with hole is  $0.02 W$

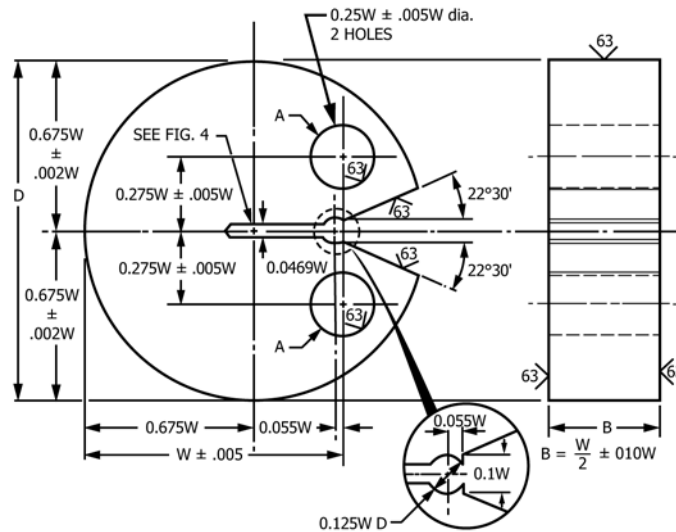
- Notes:
1. Tolerance on all dimensions  $\pm 0.013 W$
  2. Pin shall be sized so that maximum clearance with hole is  $0.01 W$



See Figure 4

- Notes:
1. Tolerance on all dimensions is  $\pm .013 W$
  2. Pin shall be sized so that maximum clearance with hole is  $.02 W$

FIG. 1 Three Compact Specimen Designs That Have Been Used Successfully for Fracture Toughness Testing

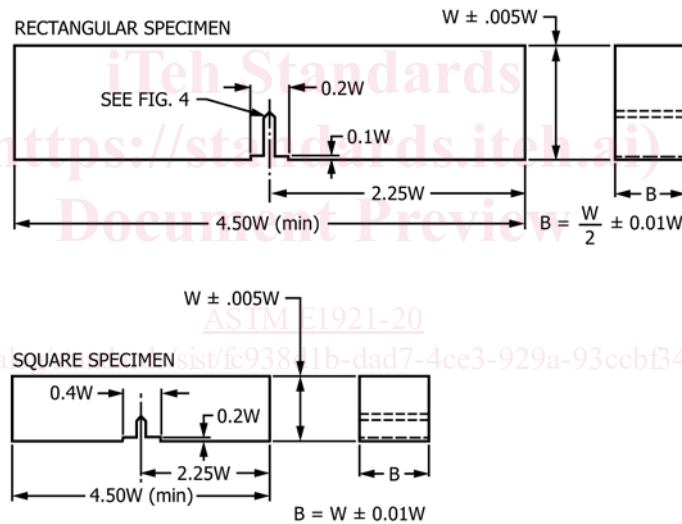


NOTE 1—A surfaces shall be perpendicular and parallel as applicable to within 0.002W TIR.

NOTE 2—The intersection of the crack starter notch tips with the two specimen surfaces shall be equally distant from the top and bottom extremes of the disk within 0.005W TIR.

NOTE 3—Integral or attached knife edges for clip gage attachment may be used. See also Fig. 6, Test Method E399.

FIG. 2 Disk-shaped Compact Specimen DC(T) Standard Proportions



NOTE 1—All surfaces shall be perpendicular and parallel within 0.001W TIR; surface finish 64v.

NOTE 2—Crack starter notch shall be perpendicular to specimen surfaces to within ± 2°.

FIG. 3 Recommended Bend Bar Specimen Design

Fig. 5 summarizes the maximum starter notch dimensions. The notch cutout for measurement gages shall be no greater than 0.2W wide by 0.1W deep. The allowable starter notch height shall be no greater than 0.063W. The centerline of the crack-starter notch shall not deviate from the specimen centerline by more than 0.005W. Fig. 5 also defines the notch tip length for both a V-notch type and a narrow-notch type. The narrow notch is often machined using a wire or plunge electrical discharge machining technique with no additional machining to further sharpen the notch root radius. Finally, Fig. 5 also summarizes the fatigue precrack extension requirements. The average length of the fatigue precrack extension from the

machined notch,  $\Delta a_{pc}$ , (determined using the measured initial crack length defined in 8.8.1) shall equal or exceed the larger of  $0.5h$ , ( $\Delta a_{sh} + \Delta a_p$ ), or 0.25 mm. Further, the sum of  $\Delta a_{pc}$  and the notch tip length shall exceed  $2.0h$ . Additional fatigue precracking requirements are contained in 7.8.

7.5 Specimen Dimension Requirements—The crack front straightness criterion defined in 8.9.1 must be satisfied. The specimen remaining ligament,  $b_o$ , must have sufficient size to maintain a condition of high crack-front constraint at fracture. The maximum  $K_{Jc}$  capacity of a specimen is given by:

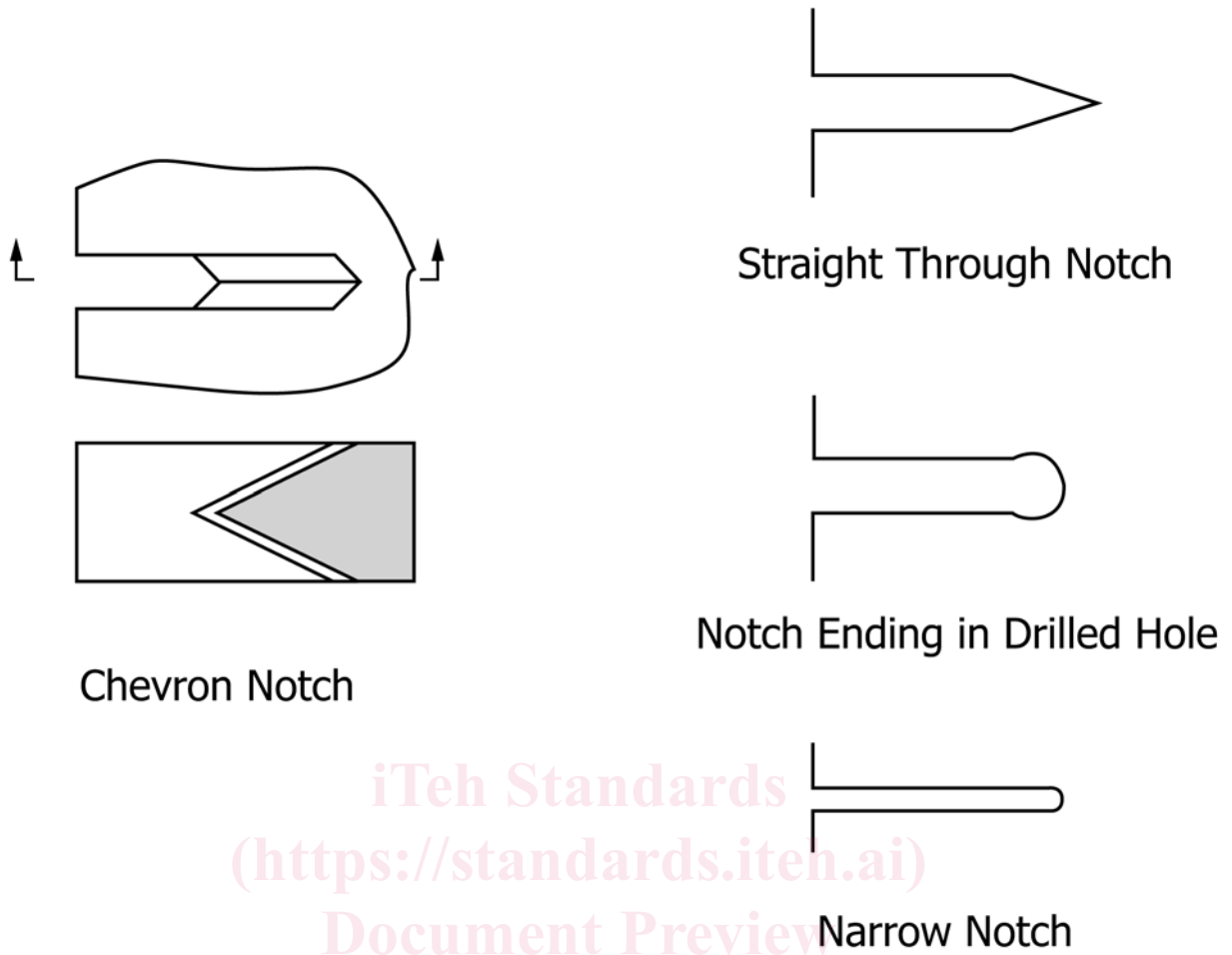


FIG. 4 Envelope Crack Starter Notches

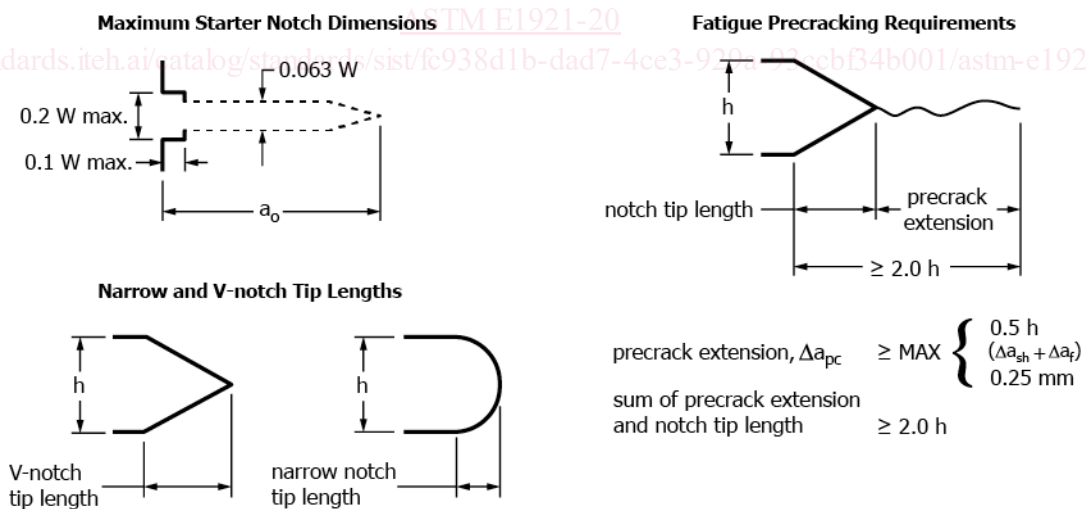


FIG. 5 Envelope of Fatigue Crack and Crack Starter Notches

$$K_{Jlimit} = \sqrt{\frac{Eb_o\sigma_{ys}}{30(1-\nu^2)}} \quad (1)$$

where:

$$b_o = W - a_o$$

Measurement of  $\sigma_{ys}$  at the test temperature ( $T$ ) using Test Methods E8/E8M is preferred for use in Eq 1. When  $\sigma_{ys}$  has not been measured at  $T$ , any of the following three methods are acceptable for estimating  $\sigma_{ys}$  at  $T$  for use in Eq 1:



(1) Using a value of  $\sigma_{ys}$  measured at a higher temperature than  $T$ .

(2) Interpolating between measurements of  $\sigma_{ys}$  at temperatures above and below  $T$ , as long as the  $\sigma_{ys}$  measurement temperatures are within 75 °C of each other. Extrapolation of the fit to infer yield strength outside of the measurement points is not allowed with this method. This method is applicable over a test temperature range of - 200 °C and 300 °C

(3) Determining  $\sigma_{ys}$  from the following equation which can be used for temperatures between -200°C and 300°C. (23) See Note 1.

$$\sigma_{ys} = \sigma_{ysRT} + 10^5(491 + 1.8 T) - 189(\text{MPa}) \quad (2)$$

where:

$T$  = test temperature (°C), and

$\sigma_{ysRT}$  = the material yield strength at room temperature (MPa)

NOTE 1—Eq 2 should not be used to determine  $\sigma_{ysRT}$  from  $\sigma_{ys}$  values obtained at other temperatures.

$K_{Jc}$  data that exceed this requirement (that is, Eq 1) are used in a data censoring procedure. Details of this procedure are described in 10.2.1.

**7.6 Small Specimens**—At high values of fracture toughness relative to specimen size and material flow properties, the values of  $K_{Jc}$  that meet the requirements of Eq 1 may not always provide a unique description of the crack-front stress-strain fields due to some loss of constraint caused by excessive plastic flow (5). This condition may develop in materials with low strain hardening. When this occurs, the highest  $K_{Jc}$  values of the data set could possibly cause the value of  $T_o$  to be lower than the value that would be obtained from testing specimens with higher constraint.

**7.7 Side Grooves**—Side grooves are optional. Precracking prior to side-grooving is recommended, despite the fact that crack growth on the surfaces might be slightly behind. Specimens may be side-grooved after precracking to decrease the curvature of the initial crack front. In fact, side-grooving may be indispensable as a means for controlling crack front straightness in bend bars of square cross section. The total side-grooved depth shall not exceed 0.25B. Side grooves with an included angle of 45° and a root radius of 0.5 ± 0.2 mm (0.02 ± 0.01 in.) usually produce the desired results.

### 7.8 Precracking:

**7.8.1 Fatigue Loading Requirements**—Allowable fatigue force values are limited to keep the maximum stress intensity factor applied during precracking,  $K_{max}$ , well below the material fracture toughness measured during the subsequent test. The fatigue precracking shall be conducted with the specimen fully heat-treated to the condition in which it is to be tested. No intermediate heat treatments between precracking and testing are allowed. There are several ways of promoting early crack initiation: (1) by providing a very sharp notch tip, (2) by using a chevron notch (Fig. 4), (3) by statically preloading the specimen in such a way that the notch tip is compressed in a direction normal to the intended crack plane (to a force not to exceed  $P_m$ ), and (4) by using a negative fatigue force ratio; for a given maximum fatigue force, the more negative the force

ratio, the earlier crack initiation is likely to occur. The peak compressive force shall not exceed  $P_m$  as defined in the equations below:

$$\text{For SE(B) specimens, } P_m = \frac{0.5Bb_o^2\sigma_Y}{S} \quad (3)$$

$$\text{For C(T) and DC(T) specimens, } P_m = \frac{0.4Bb_o^2\sigma_Y}{2W+a_o} \quad (4)$$

**7.8.2 Fatigue Precracking Procedure**—Fatigue precracking can be conducted under either force control, displacement control, or  $K$  control. If the force cycle is maintained constant, the maximum  $K$  and  $\Delta K$  will increase with crack size; if the displacement cycle is maintained constant, the reverse will happen. If  $K$  is maintained constant, force has to be reduced as a function of increasing crack size. Fatigue cycling is conducted using a sinusoidal waveform and a frequency close to the highest practical value. There is no known marked frequency effect on fatigue precrack formation up to at least 100 Hz in the absence of adverse environments. The specimen shall be accurately located in the loading fixture to achieve uniform, symmetric loading. The specimen should be carefully monitored until crack initiation is observed on one side. If crack initiation is not observed on the other side before appreciable growth is observed on the first side, then fatigue cycling should be stopped to try to determine the cause and find a remedy for the unsymmetrical behavior. Sometimes, simply turning the specimen around in relation to the fixture will solve the problem.

Precracking can be performed either by some method of smoothly and continually decreasing the maximum stress intensity factor ( $K_{max}$ ) or by using discrete steps. It is suggested that the reduction in  $K_{max}$  between any discrete step be no greater than 20 % because reducing  $K_{max}$  too rapidly can result in precrack growth rate retardation. It is also suggested that measurable crack extension occur before proceeding to the next step. Precracking is generally most effectively conducted using  $R = P_{min}/P_{max} = 0.1$ . Maximum force values shall be accurate to within ± 5 % of their target values.

Fig. 6 shows the allowable envelope for  $K_{max}$  during precracking. The precracking  $K_{max}$  and crack extension requirements are summarized in Table 1, and Table 2. Precracking can be conducted in any manner such that  $K_{max}$  remains within the envelope and the maximum fatigue force is less than  $P_m$ . The  $K_{max}$  applied to the specimen shall not exceed 25 MPa√m (22.8 ksi√in) at any crack length, and may be limited by  $P_m$  for small specimens or low yield strength materials, or both. As the testing temperature decreases compared to the precracking temperature, the warm prestressing effect increases, which can elevate the measured fracture toughness. To minimize the warm prestressing effect, the maximum  $K$  that may be applied to the specimen during  $\Delta a_f$  ( $K_f$  in Fig. 6) shall not exceed 15 MPa√m (13.7 ksi√in). Alternatively, when the testing temperature is equal to or above the precracking temperature,  $K_f$  shall not exceed 20 MPa√m (18.3 ksi√in). The minimum length of  $\Delta a_f$  (Fig. 6) is 0.2 mm (0.008 in.).  $\Delta a_{sh}$  is greater than or equal to the change in plastic zone size in going from a maximum  $K$  of 25 MPa√m (22.8 ksi√in) to  $K_f$ . The

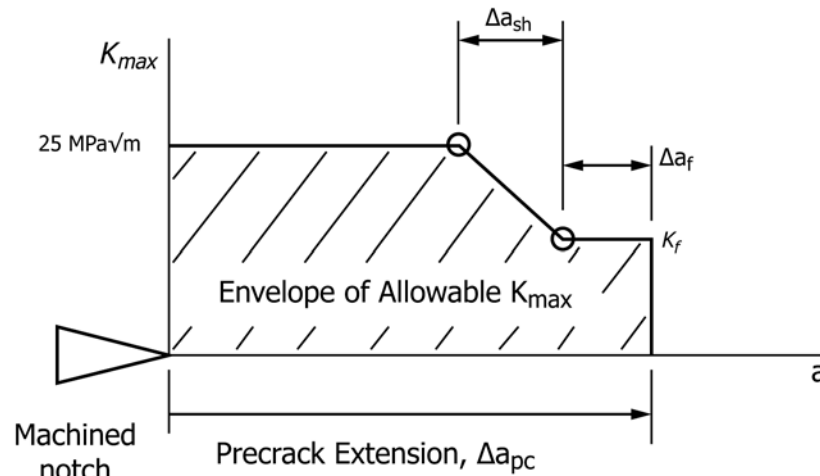


FIG. 6 Envelope of Allowable  $K_{max}$  During Precracking

TABLE 1  $K_{max}$  Requirements

Initial:  $K_{max}$  cannot exceed  $25 \text{ MPa}\sqrt{\text{m}}$  ( $22.8 \text{ ksi}\sqrt{\text{in.}}$ ) and the maximum fatigue force cannot exceed  $P_m$ .

Final:  $K_f$  depends on the test temperature:

Test Temperature	$K_f$ throughout $\Delta a_f$
< precracking temperature	< $15 \text{ MPa}\sqrt{\text{m}}$ ( $13.7 \text{ ksi}\sqrt{\text{in.}}$ )
$\geq$ precracking temperature	< $20 \text{ MPa}\sqrt{\text{m}}$ ( $18.3 \text{ ksi}\sqrt{\text{in.}}$ )

TABLE 2 Crack Extension Requirements

$$\Delta a_{pc} \geq \text{MAX} \{0.5h, (\Delta a_{sh} + \Delta a_f), 0.25 \text{ mm}\}$$

$$\Delta a_{sh} \geq r_{p1} - r_{p2}$$

Where:

$$r_{p1} = \frac{1}{3\pi} \left( \frac{K_{max}}{\sigma_{ys}} \right)^2 \text{ with } K_{max} \leq 25 \text{ MPa}\sqrt{\text{m}} (22.8 \text{ ksi}\sqrt{\text{in.}})$$

$$r_{p2} = \frac{1}{3\pi} \left( \frac{K_f}{\sigma_{ys}} \right)^2$$

$$\Delta a_f \geq 0.2 \text{ mm} (0.008 \text{ in.})$$

minimum value for  $\Delta a_{sh}$  defines the condition where the leading edge of the plastic zone remains stationary as  $K_{max}$  is decreased.

$$\Delta a_{sh} \geq r_{p1} - r_{p2} \quad (5)$$

where:

$$r_{p1} = \frac{1}{3\pi} \left( \frac{K_{max}}{\sigma_{ys}} \right)^2 \text{ with } K_{max} = 25 \text{ MPa}\sqrt{\text{m}} (22.8 \text{ ksi}\sqrt{\text{in.}})$$

$$r_{p2} = \frac{1}{3\pi} \left( \frac{K_f}{\sigma_{ys}} \right)^2$$

NOTE 2—If the yield strength ( $\sigma_{ys}$ ) is not known, a low estimate should be used to obtain a conservatively high estimate of  $\Delta a_{sh}$ .

Also, as stipulated previously in 7.4 and summarized in Fig. 5, the length of the fatigue precrack extension from the machined notch,  $\Delta a_{pc}$  (determined using the measured initial crack length defined in 8.8.1), shall equal or exceed the larger of  $0.5h$ ,  $(\Delta a_{sh} + \Delta a_f)$ , or  $0.25 \text{ mm}$  at each of the nine measurement locations defined in 8.8.1. Additionally, the sum of  $\Delta a_{pc}$  and the notch tip length shall exceed  $2.0h$  at each of the nine measurement locations defined in 8.8.1. The precrack must also meet the curvature requirement in 8.9.1. Ensuring that the average  $\Delta a_{pc}$  is long enough such that the minimum fatigue precrack extension occurs at each measurement point in 8.8.1 for a crack having the maximum curvature allowed in 8.9.1 will provide some confidence that these requirements are met before testing the specimen.

## 8. Procedure

8.1 *Testing Procedure*—The objective of the procedure described here is to determine the  $J$ -integral at the point of crack instability,  $J_c$ . Crack growth can be measured by partial unloading compliance, or by any other method that has precision and accuracy, as defined below. However, the  $J$ -integral is not corrected for slow-stable crack growth in this test method.

8.2 *Test Preparation*—Prior to each test, certain specimen dimensions should be measured, and the average starting crack size estimated. The average starting crack size can be estimated using a variety of techniques including precrack compliance, back-face strain, and using the average of the optical side face measurements.

NOTE 3—When side-grooving is to be used, first precrack without side grooves and then visually estimate the precrack size.

If estimates are available from multiple techniques, the user shall select the value that is believed to be most representative of the average crack size.

8.2.1 The dimensions  $B$ ,  $B_N$ , and  $W$  shall be measured to within 0.05 mm (0.002 in.) accuracy or 0.5 %, whichever is larger.

8.2.2 Follow Test Method E1820, 8.5 for crack size measurement, 8.3.2 for testing compact specimens and 8.3.1 for testing bend specimens.

8.3 The required minimum number of  $K_{Jc}$  results that are uncensored is specified according to the value of  $K_{Jc(med)}$ . See also 8.5.

8.4 *Test Temperature Selection*—It is recommended that the selected temperatures be close to that at which the  $K_{Jc(med)}$  value will be about 100 MPa√m for the specimen size selected.

8.4.1 *Quasi-static loading rates*—If loading rate complies with the limits stated in 8.7.1, Charpy V-notch data can be used as an aid for predicting a viable test temperature. If a Charpy transition temperature,  $T_{CVN}$ , is known corresponding to a 28 J Charpy V-notch energy or a 41 J Charpy V-notch energy, the constant  $C$  can be chosen from Table 3 corresponding to the test specimen size (defined in 3.3.19), and used to estimate<sup>5</sup> the test temperature from (12, 24).

$$T = T_{CVN} + C \quad (6)$$

<sup>5</sup> Standard deviation on this estimate has been determined to be 15°C.

**TABLE 3 Constants for Test Temperature Selection Based on Charpy Results**

Specimen Size, ( $nT$ )	Constant C (°C)	
	28 J	41 J
0.4 <sup>A</sup>	–32	–38
0.5	–28	–34
1	–18	–24
2	–8	–14
3	–1	–7
4	2	–4

<sup>A</sup> For precracked Charpy specimens, use  $C = -50$  or  $-56^\circ\text{C}$ .

8.4.2 The procedure outlined in 8.4.1 is only appropriate for determining an initial test temperature. The iterative scheme described in 10.3.1 may be necessary to refine this test temperature in order to increase  $T_o$  accuracy. Testing below the temperature specified in Eq 6 may be appropriate for low upper-shelf toughness materials to avoid ductile crack growth before cleavage onset, and for low yield strength materials to avoid obtaining data that must be censored because it exceeds  $K_{Jc\text{limit}}$  in accordance with Eq 1.<sup>6</sup>

8.5 *Testing Below Temperature,  $T_o$* —When the equivalent value of  $K_{Jc(med)}$  for 1T specimens is greater than 83 MPa√m, the required number of uncensored  $K_{Jc}$  values to perform the analyses covered in Section 10 is six. However, small specimens such as precracked Charpy specimens can develop excessive numbers of  $K_{Jc}$  values that exceed the  $K_{Jc\text{limit}}$  (Eq 1) when testing close to the  $T_o$  temperature. In such cases it is advisable to test at temperatures below  $T_o$ , where most, if not all,  $K_{Jc}$  data developed can be uncensored. The disadvantage here is that the uncertainty in  $T_o$  determination increases as the lower-shelf toughness is approached. This increase in uncertainty can be countered by testing more specimens thereby increasing the  $K_{Jc(med)}$  accuracy. The number of specimens required for obtaining a valid  $T_o$  measurement as a function of the test temperature is provided in 10.3 (10.4.1 for the special case of testing at a single temperature).

8.6 *Specimen Test Temperature Control and Measurement*—For tests at temperatures other than ambient, any suitable means (liquid, gas vapor, or radiant heat) may be used to cool or heat the specimens, provided the region near the crack tip can be maintained at the desired temperature as defined in 6.7 during the conduct of the test.

8.6.1 The most dependable method of monitoring test temperature is to weld or spot weld each thermocouple wire separately to the specimen, spaced across the crack plane. The specimen provides the electrical continuity between the two thermocouple wires, and spacing should be enough not to raise any question of possible interference with crack tip deformation processes. Alternative attachment methods can be mechanical types such as drilled hole, or by a firm mechanical holding device so long as the attachment method is verified for accuracy and these practices do not disturb the crack tip stress field of the specimen during loading.

8.6.2 To verify that the specimen is properly seated into the loading device and that the clip gage is properly seated, estimate the specimen crack size while working-in the test setup at test temperature. Working-in is accomplished via repeated preloading and unloading in the linear elastic range between force values of 0.2  $P_{max}$  and  $P_{max}$  (where  $P_{max}$  is the largest allowable precracking force of the finishing cycles as prescribed in 7.8.2) at least three times. For each unloading/reloading sequence, estimate the precrack size using Test Method E1820, Eq A2.12 for C(T) specimens and Eq A1.12 for SE(B) specimens. The elastic modulus,  $E$ , used in these calculations shall be the nominal value for the material at the test temperature. The nominal value of  $E$  shall come from

<sup>6</sup> Data censoring is covered in 8.9.2 and Section 10.

either handbook values or dedicated modulus testing per Test Method E111 or equivalent. Tensile test results do not provide accurate elastic modulus values. Alternatively, the following equation can be used to determine the nominal value of  $E$ .

$$E = 204 - T/16 \text{ GPa} \quad (7)$$

where:

$T$  = test temperature in °C.

This equation was derived from fitting the tabular values for ferritic steels contained in ASME Section II, Part D. The fit is valid for  $-200^\circ\text{C} \leq T \leq 300^\circ\text{C}$ .

8.6.3 Check the estimated crack size slope against the average precrack size defined in 8.2. The test setup is considered acceptable when the last three consecutive estimated crack sizes are all within 10 % of the final precrack size and no individual estimated crack size differs from the mean by more than  $\pm 0.002W$ . To minimize the difference between the precrack size and the working-in estimated crack size, the nominal  $E$  value may be adjusted up to 10 %. Modulus adjustments should only be made when the force transducer and clip gage calibrations are known to be within acceptable limits of accuracy, see Section 6. The value of  $E$  in use for the final three acceptable working-in unloading/reloading sequences shall be used for all crack size estimates throughout the remainder of the given test. If the repeatability or the accuracy, or both of the estimated crack sizes are outside the prescribed limits, the test setup is questionable and should be thoroughly rechecked. It is essential that the specimen temperature and clip gage are stable and that the clip gage knife edges are sharp in order to meet these requirements. Be aware that ice buildup at the loading clevis hole between tests can affect accuracy. Therefore, the loading pins and devices should be dried before each test.

8.7 *Testing for  $K_{Jc}$* —All tests shall be conducted under displacement control. Force versus load-point displacement measurements shall be recorded. Periodic partial unloading can be used to determine the extent of slow-stable crack growth if it occurs. Alternative methods of measuring crack extension, for example the potential drop method, can be used (21). If displacement measurements are made at a location other than at the load point, the ability to infer load point displacement within 2 % of the absolute values shall be demonstrated. In the case of the front face for compact specimens (7.1), this requirement has been sufficiently proven so that no demonstration is required. For bend bars, see 6.5.2. Crack size prediction from partial unloading slopes at a different location will require different compliance calibration equations than those recommended in 8.6.2. Table 2 in Practice E561 contains equations that define compliance for other locations on the compact specimen.

8.7.1 *Quasi-static Loading*—Load specimens at a rate such that  $\dot{K}$  during the initial elastic portion is between 0.1 and 2 MPa $\sqrt{\text{m/s}}$ . Variation of the loading rate within these limits allows obtaining a  $T_o$  which is insensitive to the loading rate within 10°C (25). The testing machine loading rate associated with this allowable range can be determined in terms of the time to reach  $P_m$  ( $t_m$ ) or the specimen load-line displacement rate  $\dot{\Delta}_{LL}$ . Table 4 is provided to determine the time to  $t_m$  or  $\dot{\Delta}_{LL}$  as a function of  $\dot{K}$ ,  $W$ ,  $E$ , and  $\sigma_{YS}$  for each allowable specimen

**TABLE 4 SE(B) Specimen Rate Estimation-C(T) Specimen Rate Estimation**

SE(B) Specimen Rate Estimation			C(T) Specimen Rate Estimation		
$a/W$	$\frac{t_m \dot{K}}{\sigma_{YS} \sqrt{W}}$	$\frac{E \dot{\Delta}_{LL}}{dK/dt \sqrt{W}}$	$a/W$	$\frac{t_m \dot{K}}{\sigma_{YS} \sqrt{W}}$	$\frac{E \dot{\Delta}_{LL}}{dK/dt \sqrt{W}}$
0.45	0.346	5.064	0.45	0.412	3.475
0.50	0.333	5.263	0.50	0.386	3.829
0.55	0.318	5.522	0.55	0.361	4.212
0.60	0.302	5.851	0.60	0.336	4.635
0.65	0.283	6.267	0.65	0.312	5.118
0.70	0.263	6.798	0.70	0.287	5.696

geometry.  $P_m$  is nominally 40 % of limit force; see 7.8.1. The actual crosshead rate used must be adjusted to account for test machine compliance if the load-line displacement rate of Table 4 is used. The crosshead speed during periodic partial unloadings, if applied, may be as slow as needed to accurately estimate crack growth, but shall not be faster than the rate specified for loading.

8.7.2 *Slow Loading Rates*—For loading rates less than 0.1 MPa $\sqrt{\text{m/s}}$ , the procedures of this test method can be used if the failure mode remains cleavage. The corresponding reference temperature is then reported as  $T_{o,X}$  using the convention described in A1.2.1.1.

8.8 *Test Termination*—After completion of the test, optically measure initial crack size and the extent of slow-stable crack growth or crack extension due to crack pop-in, or both, when applicable.

8.8.1 When the failure event is full cleavage fracture, determine the initial fatigue precrack size,  $a_o$ , as follows: measure the crack size at nine equally spaced points centered about the specimen centerline and extending to 0.01 $B$  from the free surfaces of plane sided specimens or near the side groove roots on side grooved specimens. Average the two near-surface measurements and combine the average of these two readings with the remaining seven crack measurements. Determine the average of those eight values. Measure the extent of slow-stable crack growth if it develops applying the same procedure. The measuring instruments shall have an accuracy of 0.025 mm (0.001 in.).

8.8.2 *Post-Test Check*—Compare the estimated fatigue precrack length determined in 8.6.3 with the optical average value determined in 8.8.1. The pre-test estimate shall not differ from the post-test optical value by more than 5 %. If the error exceeds 5 %, then a unique value of  $E$  ( $E_i$ ) can be found for each test to match the optical average value as closely as possible using Test Method E1820, Eq A2.12 for C(T) specimens and Eq A1.12 for SE(B) specimens.  $E_i$  values shall be within 10 % of the nominal value of  $E$  identified in 8.6.2.

8.9 *Qualification of Data:*

8.9.1 The  $K_{Jc}$  datum shall be considered invalid if any of the nine physical measurements of the starting crack size differ by more than  $0.1(b_o B_N)^{1/2}$  from the average defined in 8.8.1. The datum is also invalid if the calculated crack length for the test determined in 8.8.2 differs from the optical average value determined in 8.8.1 by more than 5 %.